Indirect Impulse Bit Measurement For A Quasi-Steady MPD With Applied Magnetic Field

IEPC-2009-225

Presented at the 31st International Electric Propulsion Conference,
University of Michigan, Ann Arbor, Michigan, USA
September 20–24, 2009

Francesco Guarducci[*], Jan Lehnert[†] and Giorgio Paccani[‡]
Sapienza Università di Roma, 00185, Roma, Italia

Abstract: Impulse bit measurement of a quasi-steady Teflon® propellant MPD with applied magnetic field is the focus of this paper. Thrust Stand technique has proved to be satisfactory when operating in self-field-only mode, but presents some uncertainties while operating in applied-field mode: a magnetic coupling between the coil and the laboratory facility resulting in TS displacement has been observed. This phenomenon and its consequences on measurements have been investigated. A TS calibration approach has been carried out as a first attempt to take into account the magnetic coupling disturb. Insufficient theoretical evidence on calibration as the right way of proceeding led to the introduction of the target technique: a suitable target used as a ballistic pendulum can be a straightforward solution to the magnetic coupling problem. Experiments have been carried out for a range of firing energies (2000 to 3000 J) and applied magnetic field intensities (0.03 to 0.16 T): results are hereafter presented.

Nomenclature

A	= oscillating system amplitude
B	= magnetic field
E_0	= initial energy stored in the PFN
I_{bit}	= impulse bit
l	= pendulum length
m	= mass
μ_0	= vacuum magnetic permeability
τ	= discharge duration
ω	= oscillating system pulse frequency
v	= velocity

Subscript

an	= anodic
cat	= cathodic
eq	= equivalent
r	= rotating
Reg	= obtained through Regression method
t	= translating

[*]PhD Student, Scuola di Ingegneria Aerospaziale, Roma, francesco.guarducci@gmail.com
[†]Undergraduate Student, Facoltà d'Ingegneria, lehnert.jan@gmail.com
[‡]Senior Researcher, Department of Mechanics and Aeronautics, giorgio.paccani@uniroma1.it.

I.   Introduction

THIS paper deals with an experimental analysis of a solid propellant (Teflon®) quasi steady Magnetoplasmadynamic (MPD) thruster, which can operate both in applied-field and self-field mode. It is well known that applying an external axial magnetic field to a self-field MPD improves thruster performances, in terms of thrust and efficiency. It has already been shown that this procedure causes a steadier arc and a more uniform discharge (increasing repeatability as well), possibly reducing cathode erosion. The purpose of this work is to examine and compare different indirect impulse bit measurement techniques, with particular focus on method reliability in the applied-field operation mode: in fact, it has been noticed also by other authors that the applied field could affect measuring systems introducing noise and biases. The different techniques for thrust measurements employed at the Electric Propulsion Laboratory of the University of Rome "La Sapienza", are intended to be a simple (and cheap) way to seek out these effects and find a reasonable range for thrust performance of an applied-field MPD, without recurring to very expensive devices. This is indeed part of an effort, still in progress, to find a feasible, reliable and effective low-cost method for thrust measurements.

II.   Experimental Apparatus

A.   The propulsive system

The thruster used in the La Sapienza Electric Propulsion Laboratory is a coaxial, quasi-steady MPD, with radially set-and-fed bar-shaped solid propellant (Teflon), named Mira C (Fig. 1). The thruster
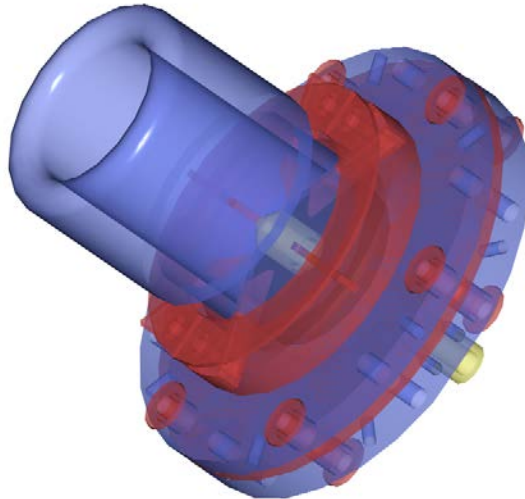

Figure 1. 3D rendering of Mira C thruster.

copper cathode has a truncated cone shape, with a maximum diameter of 18 mm; the anode instead, which operates also as discharge and acceleration chamber, is an aluminum cylinder with an internal diameter of 60 mm. The thruster is operated in pulsed regime; each pulse has a quasi stationary phase of about 1 ms. The energy is supplied by a 12 electrolytic capacitors PFN, with a total capacitance of about 63 mF and a maximum charge voltage of 450 V. Experiments have been carried out at different PFN charge voltage, in order to have a stored energy per shot varying in the 2000 J - 3000 J range; more precisely 2000 J, 2333 J, 2666 J and 3000 J values have been considered. A solenoidal electromagnet has been mounted coaxially to the thruster, surrounding the entire discharge region, providing an axial magnetic field component. The magnetic coil is powered by a capacitive PFN, designed to obtain current pulses with a steady state phase lasting for a time longer than the thruster shot time, with a maximum magnetic field on the axis of about 0.5 T; a suitable device synchronizes thruster and magnet pulses, so that the thruster shot occurs during magnet steady phase. The electromagnet PFN has been charged at 5 different potential values, in order to generate a magnetic field of respectively 0.031 T, 0.058 T, 0.092 T, 0.125 T and 0.159 T. For each stored energy level tests have been performed with each of these five field levels, in addition to the thruster self-field mode. The tests have been carried out inside a 0.7 m diameter and 1.3 m length vacuum chamber, with a back pressure as low as 10^{-5} mbar.

B. Electrical parameters and preliminary remarks

In order to monitor the discharge behaviour, current and voltage time history during the pulse has been acquired; the electrodes potential difference is measured directly by an oscilloscope and current through a Rogowsky coil.

A higher discharge repeatability and stability are observed in applied magnetic field thruster operation (Fig. 2); as already pointed out, this is indeed one of the most pronounced effects of axial field application. Moreover, simple computer elaboration of the collected data allows to evaluate the current parameter:
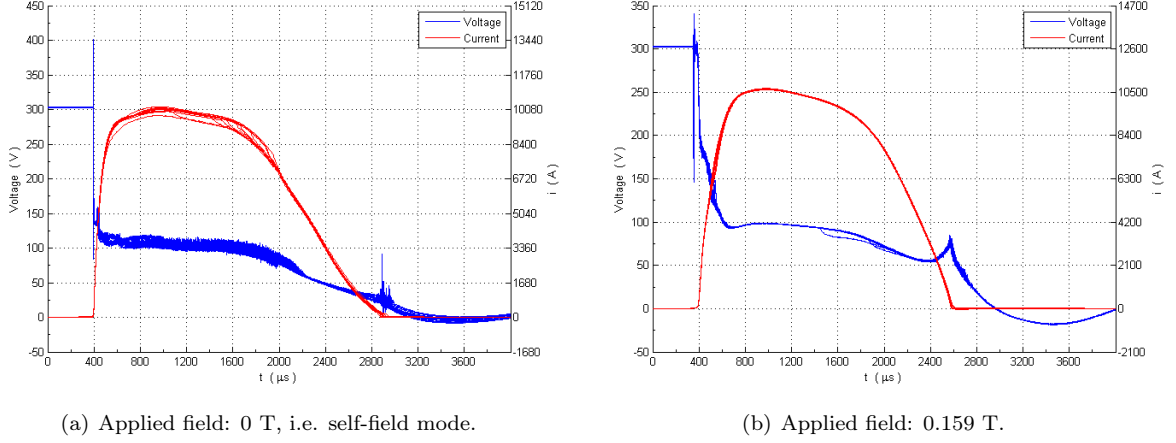

(a) Applied field: 0 T, i.e. self-field mode.

(b) Applied field: 0.159 T.

Figure 2. Current and voltage in 12 different shots at 3000 J for different applied field intensities.

$$\Psi = \int_0^\infty i^2(t)\ \mathrm{d}t \tag{1}$$

Figure 3 (a) shows the trend of discharge duration τ with applied magnetic field for thruster operating at different energies; it is remarkable that the higher is the magnetic field the shorter this time becomes; this effect is even more evident in Fig. 3 (b), where the two Fig. 2 (a) and 2 (b) have been overlaid. Here
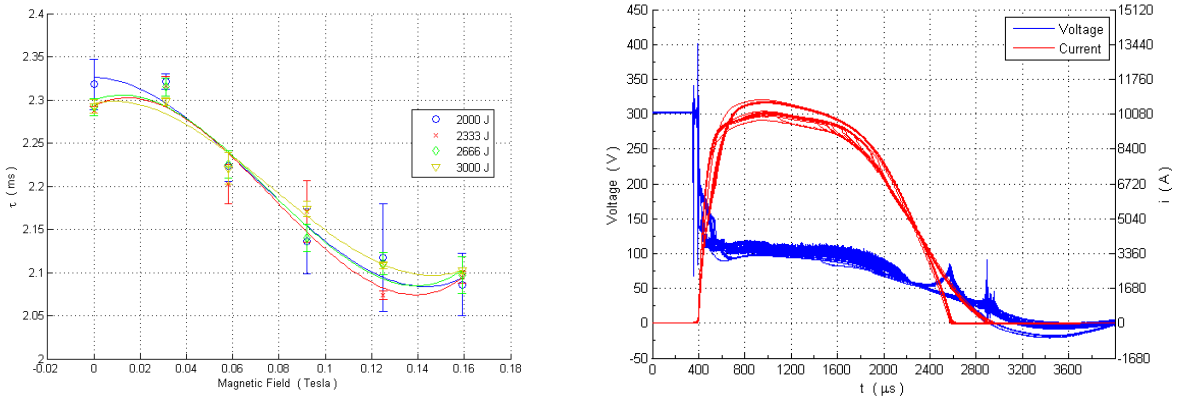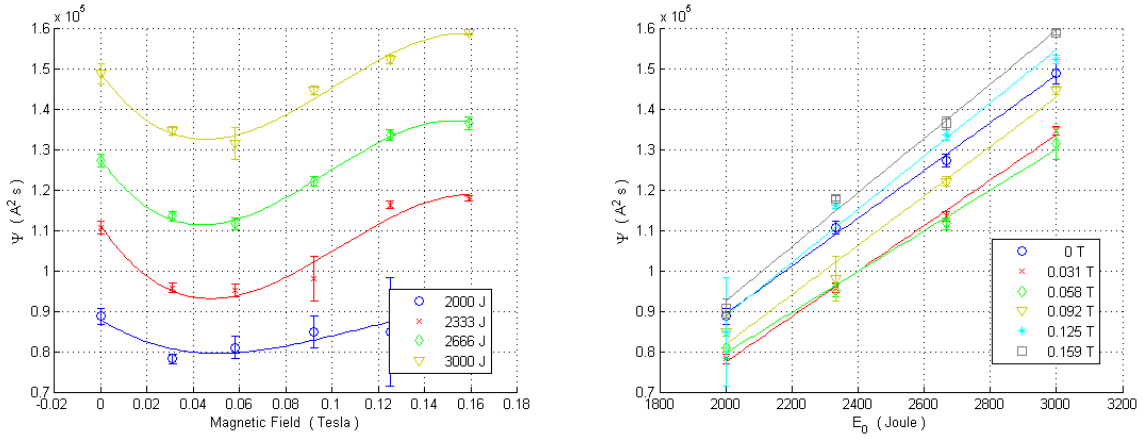

(a) τ trends for different initial energies versus applied field value.

(b) Visual evidence of discharge time reduction with increasing applied field value.

Figure 3. Discharge time variations evaluated through τ parameter and visual inspection.

it becomes also clear that at higher magnetic field levels the current reaches higher maximum values. The discharge duration τ may be influenced in terms of discharge position on the electrodes: the applied field pushes the discharge towards the edge of the discharge chamber, so that eventually the discharge could be "blown" away. Next are shown the current parameter trends versus both the energy stored in the PFN (E_0) and the applied magnetic field. The current parameter has, as it was expected, a linear dependency on E_0, otherwise it shows a little decrement for low applied magnetic field, increasing its value again for higher field. The current parameter allows to obtain an impulse estimate through Maecker's formula:[1]

$$I_{bit} = \mu_0 \ln \frac{r_{an}}{r_{cat}} \Psi \tag{2}$$

(a) Ψ trends for different applied field values versus initial energy value.

(b) Ψ trends for different initial energy values versus applied magnetic field value.

Figure 4. Ψ trends plotted with respect to operation parameters variation.

where r_{cat} and r_{an} are the cathode and anode radii.

Unfortunately this formulation is valid only for self-field thrusters, because it doesn't take into account the contributions to thrust given by the applied magnetic field through a supplementary "pumping term" and the partial conversion in axial kinetic energy of azimuthal kinetic energy. The only way Maecker's formula is affected by applied magnetic field is through the variations it causes to the current parameter.

III.   Thrust Stand Impulse Bit Measurements

A.   The thrust Stand Technique

A pendulum-based Thrust Stand technique has proved suitable for thrust measurement purpose;[2,3] for pulsed-operated devices this technique allows to evaluate the total impulse rather than the instantaneous thrust. TS theory is based on a simple pendulum model; let's assume this has a mass m and let's introduce some features of real systems, such as a damping factor c' and an elastic force with constant k', allowing to model the real hinge and any other phenomenon responsible for oscillation damping. Moreover, for small displacements the angular deflection can be linearized and expressed in terms of linear displacement. From the harmonic oscillator equation for a single degree of freedom system, and with the hypothesis that the initial velocity is a consequence of an instantaneous impulse transferred by the thruster to the TS in the direction of motion ($I = mv$), a simple equation for the pendulum Thrust Stand motion is found:

$$x(t) = Ae^{-\alpha t}\sin(\omega t + \varphi), \tag{3}$$

which leads to a simple impulse formula:

$$I = mA\omega, \tag{4}$$

where A is the maximum displacement of the undamped harmonic oscillator.

In order to exploit this result for a real system, the device to be used must match some requirements: it has to be as close as possible to a one-degree-of-freedom system, then without rotating masses. Several solutions have been adopted in different laboratories, including simple pendulum and inverted pendulum (simple or with multiple arms): the choice is usually made depending on facility needs and capabilities.[3–6] The TS used for our tests is a double parallelogram linkage with four rods connecting a plate to a fixed structure (Fig. 5). Since the only degree of freedom should be in the direction of motion, the rods are connected in a triangular shape which should not allow transverse oscillation and make the whole structure stiffer. Each of the eight hinges consists of a bronze sheet spring. The thruster is then mounted on the plate. To avoid hard wire damping and electrodynamical forces biasing the TS motion, the connection to the power supply is obtained by means of electrodes dipped in coaxial mercury pots, so that the whole power line is coaxial.[2,3] For small deflection angles the motion of the plate/thruster complex is a simple translation that has been measured with an optical sensor pointing the base plate. *The sensor signal is picked up by an oscilloscope, then the acquired data are saved to a computer where they are later processed. The optical sensor is characterized by a nominal resolution of 1 μm, high linearity and a 40 kHz sample rate; the oscilloscope is set to register 8192 samples in a 16 s measuring*
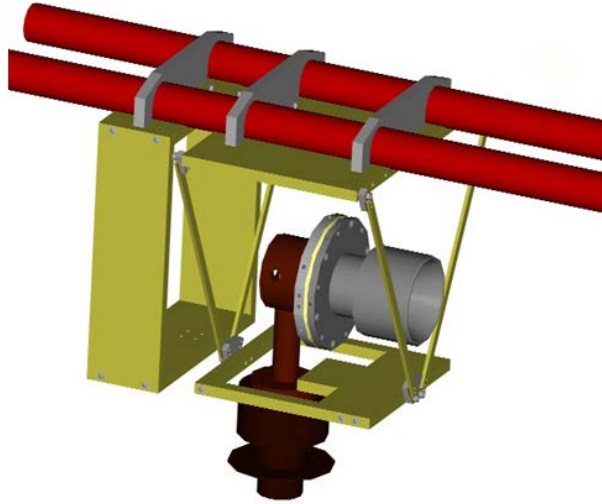
Figure 5. Thrust Stand device rendering.

window.

The term m in Eq. (4) has to be slightly modified in order to compensate the lapse between the model and the real device, which actually has rotating masses. An equivalent mass m_{eq} can be then defined as the mass that should belong to a simple pendulum (with an elastic hinge), with the same length as the TS, and with the elastic constant of the hinge equal to TS springs' stiffness, in order to make it dynamically equivalent to the TS, i.e. characterized by the same natural angular frequency.

A Lagrangian model has been developed to find the analytical expression for TS angular frequency. It considers separately the TS's translating mass (mass of the thruster plus the base plate complex), m_t, and the rotating mass, namely the mass of the rods, m_r.[9] Stating equality between this angular frequency and the simple pendulum one and solving for the equivalent mass it is found that

$$m_{eq} = \frac{\frac{1}{3}m_r + m_t}{1 + \frac{1}{6}\frac{m_r g}{k'l}} \simeq \frac{1}{3}m_r + m_t, \tag{5}$$

where the term $\frac{m_r g}{6k'l}$ has been cancelled, as it is negligible according to experimental values.

B.   Total Impulse Measurement

The Impulse for each shot, I_{bit}, is calculated with Eq. (4), where m is replaced by m_{eq}. TS's angular frequency has been measured through frequency analysis of the displacement signal: ω simply is the frequency corresponding to the Power Spectral Density (PSD) global maximum. *The value of ω has been calculated for each measure, and proved to be stable at 1.75 Hz.*

The term A is the maximum displacement of the undamped harmonic oscillator: the actual system nevertheless, presents a noticeable damping. Equation (4) stays valid for damped systems when A assumes the meaning of the initial value of Eq. (3) envelop, given by the expression:

$$\hat{x}(t) = \frac{I}{m\omega}e^{-\alpha t}. \tag{6}$$

Thus:

$$\hat{x}(0) = \frac{I}{m\omega} = A. \tag{7}$$

In order to estimate the value of A different displacement curve analysis methods have been developed.

1.   Exponential Regression Method

Starting from Eq. (3) and (6) A is the displacement curve envelop value at firing time. This envelop is obtained performing the curve peaks exponential regression (Fig. 6). This is true as long as the TS is assimilable to a one-degree-of-freedom system. Signal to noise ratio suggests not to take into account the latter part of the window: the exponential regression is calculated over the first half of the peaks, hence the trend shown in Fig. 6 where the red curve does not fit the last peaks very well. There is a
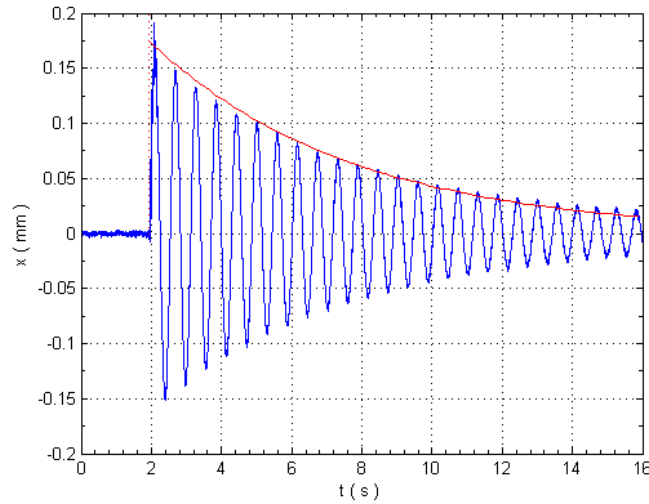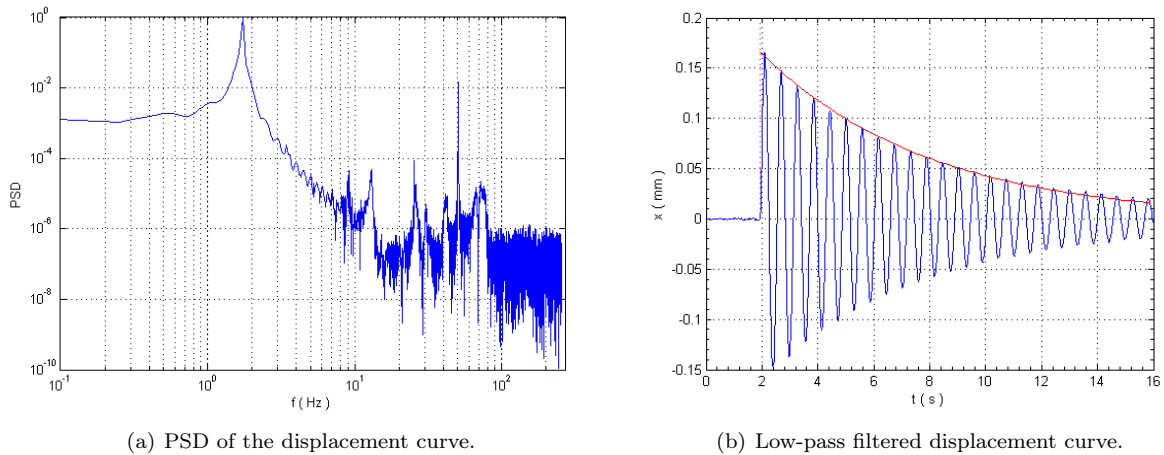
Figure 6. TS displacement curve.

fitting problem also for the first maximum.

Indeed the model employed so far is based on a one-degree-of-freedom system hypothesis. Such a system's displacement curve should have a Power Spectral Density (PSD) presenting just a single peak centered on its natural frequency. In a multiple-degrees-of-freedom system power is distributed over multiple frequencies, multiple peaks are visible, every natural mode seen in the PSD having an amplitude of its own. Analyzing the (normalized) power spectral density of the displacement curve (Fig. 7 (a)), multiple resonance peaks can be detected: the first and principal one is related to the pendulum-like motion the TS has been designed to have; a strong peak is found at 50 Hz, and it is always filtered out, because it can be easily identified as electric line noise. The others can be regarded as resonance peaks of superior

(a) PSD of the displacement curve.

(b) Low-pass filtered displacement curve.

Figure 7.

modes: even if these peaks are at least more than three orders of magnitude smaller than the first one, they imply that the TS is not a one-degree-of-freedom system. It can be observed that higher frequency modes are quickly dumped. This means that successive peaks of the displacement curve are less and less affected by these modes. As the regression method takes into account many peaks after the first one, it already gives superior weight to the first frequency rather than to superior ones. Nonetheless the first peak excessive amplitude affects the measurement, so that a low-pass filtering (cut frequency 15 Hz) has been applied. After filtering the interpolation is much more precise, especially for the first peak as shown in Fig. 7 (b).

Through high frequency modes filtering, the amplitude A has been obtained in accordance with the single-degree-of-freedom model, excluding non idealities present in the actual TS device. Such a procedure, though, doesn't analyze the physical meaning of the non idealities themselves: any displacement

contribution beside the principal mode does not belong to the one-degree-of-freedom model, but this does not imply it is not related to a thrust contribution. The TS structure, as any mechanical device, has several elastic modes, some of which may be in the thrust direction, while others may be transverse or torsional in the base plate plane. The sheet springs presence suggests that a higher frequency (vibrational) axial mode is present: thus complete low pass filtering could leave out a small but valuable impulse component.

2. Maximum Peak Method

The simplest (intuitive) estimate of A can be the value of the displacement curve maximum peak. The main issue with this approach is that a damped system is dealt with: in the first quarter of period motion has already been damped, so the maximum displacement measured should be lower than that of a corresponding undamped system. Nevertheless the first peak contains information about high frequency vibrations that may be related to an impulse component. This is proved by the fact that low-pass filtering leads to convergence of Regression and Maximum Peak methods.

3. Methods comparison and the Maecker reference

To investigate which of the two methods presented is more suitable for impulse measurements, it is useful to compare their trends for self-field thruster operation with the Maecker's equation curve given by the corresponding current data (Fig. 8). It is evident that the regression method curve very closely follows Maecker's: this could mean that higher frequency modes seen before in Fig. 7 (a) possibly are not directly related to thrust production, possibly depending on thruster misalignment on the stand, or stand itself dynamics. Thus in the following the collected experimental impulse bit measurements will be obtained by the exploitation of the regression method.
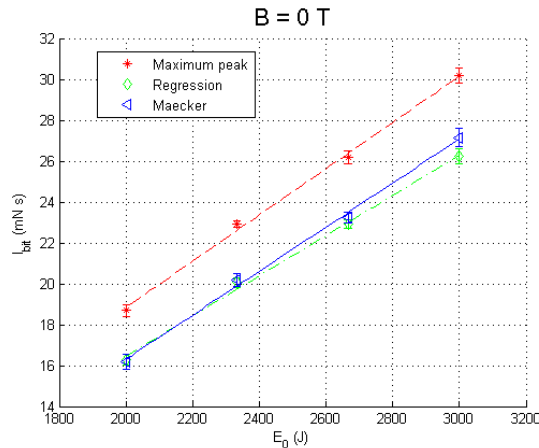

Figure 8. Impulse Bit obtained through Regression Method, Maximum Peak Method and Maecker Formula.

C. Experimental Results

As it has been introduced before, the thruster has been operated at a variety of energy levels and both in self-field and applied-field mode; more precisely five field intensities have been investigated, apart from the 0 T level of the self-field mode. For each couple of energy and field values at least 12 tests have been accomplished, so that the impulse measurements that will be presented in the next plots result from the mean of impulses calculated from single shots.

The applied field influence on the propulsive system has been pointed out using the energy stored in the PFN (E_0) as the independent variable. The impulse bit versus the energy stored in the PFN has, as it was expected, a strongly linear trend (Fig. 9 (a)); this characteristic is not even affected by magnetic field, whose effect appears to be an increase in impulse bit value, almost independent on thruster energy level. Figure 9 (b) shows impulse bit trends for increasing axial magnetic field: it is remarkable that impulse bit appears to be negatively affected by the application of a low magnetic field; nevertheless for larger magnetic field values, the impulse bit is positively affected as it was predicted by the theory;[1] anyway the trends present an optimum value for magnetic field around 0.125 T, where the measured impulse bit reaches a maximum, beginning thereafter to decrease once again with increasing magnetic field. These
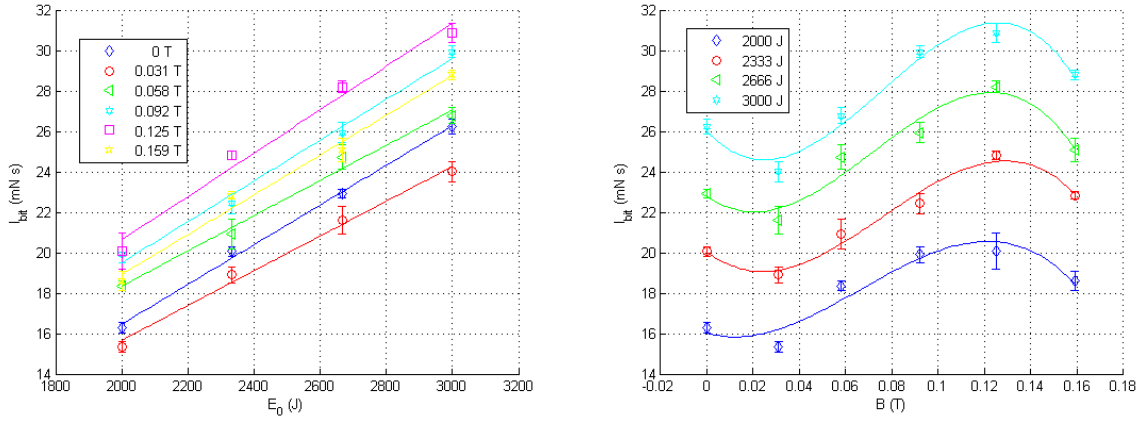
(a) I_{bit} versus initial energy E_0 for each applied B field value. (b) I_{bit} versus applied B field for each initial energy E_0 value.

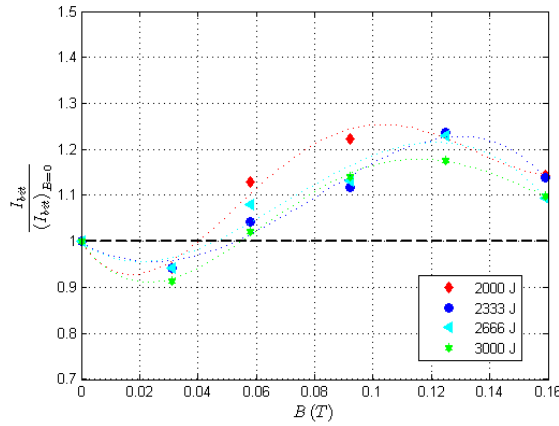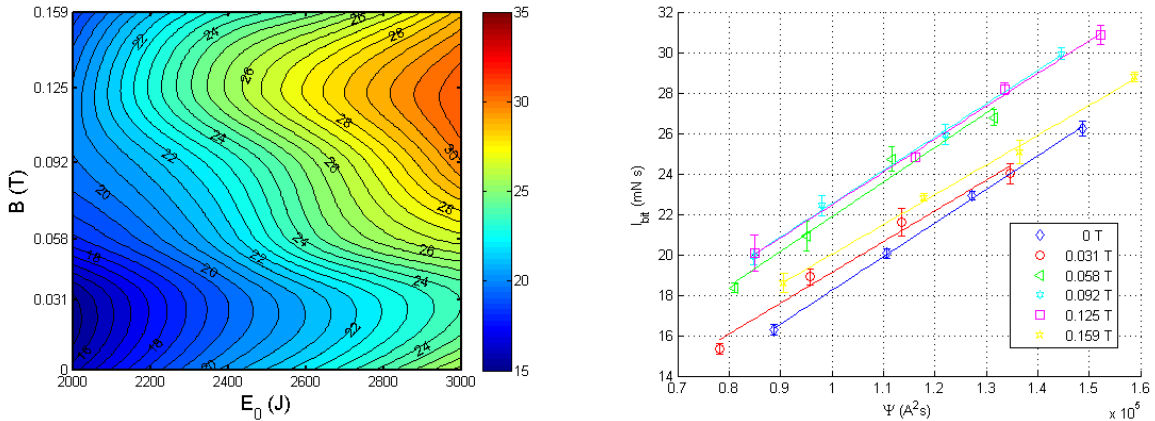**Figure 9.** I_{bit} **trends versus operation parameters.**

Figure 10. $I_{bit}/(I_{bit})_{B=0}$ **versus applied field value.**

(a) I_{bit} versus both applied B field and initial energy E_0. 　　　(b) I_{bit} trend versus Ψ.

Figure 11.

conclusions are supported by Fig. 10: here the ratio between impulse bit measurements for applied-field mode and impulse bit for self-field mode thruster operation are presented for increasing magnetic field values: similar behavior has been noticed also by other authors.[7] This phenomenon has been explained by the tendency of the discharge to move towards the nozzle exit for increasing values of the applied

magnetic field. Figure 11 (a), at last allows an immediate visualization of the impulse bit as a function of both magnetic field and PFN stored energy. The magnetic field effect on the thruster's behaviour has been put in evidence assuming the current parameter Ψ as the independent variable (Fig. 11 (b)). Because of the linear dependence between Ψ and E_0 the impulse bit shows again a linear trend.

Another interesting parameter that can be analyzed is the ratio between the impulse bit measured by the thrust stand and the impulse estimated through the Maecker formula. Fig. 12 shows this parameter as a function of magnetic field for different energy levels: as it was stated before, the only way Maecker's formula is affected by applied magnetic field is through the variations it causes to the current parameter, neglecting any other thrust contribution; it is remarkable that also this ratio indicates that there is an optimum magnetic field value between 0.092 T and 0.125 T where these magnetic field extra-contribution to thrust reach their extreme value, becoming soon smaller for magnetic field values over 0.125 T.
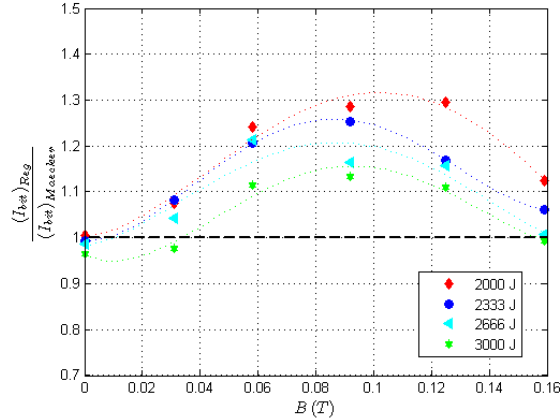

Figure 12. $(I_{bit})_{Reg}/(I_{bit})_{Maecker}$ **versus applied field value.**

D.   Thrust Stand Calibration - Experimental Results

It has been observed that the magnet, which is operated in pulses few hundreds milliseconds long, produces a magnetic coupling between the thrust stand/thruster complex and the vacuum facility's ferromagnetic components. This effect results in a magnetically forced displacement, completely independent of the thruster impulse, as the oscillations measured with the magnet operated alone prove. This problem has been experienced also by other authors and solved with different techniques[3,6]. Some researchers measured this effect aside from thruster firing, thus obtaining tares which were later subtracted from thrust measurements[3]; others chose an active damping solution: the initial displacement caused by the electromagnet has been damped before igniting the thruster[6]. The latter solution is feasible for steady-state thrusters, while for pulsed operation, where the electromagnet is working for few hundreds of milliseconds, it becomes inapplicable. The tares approach has been tried, even if there is no physical
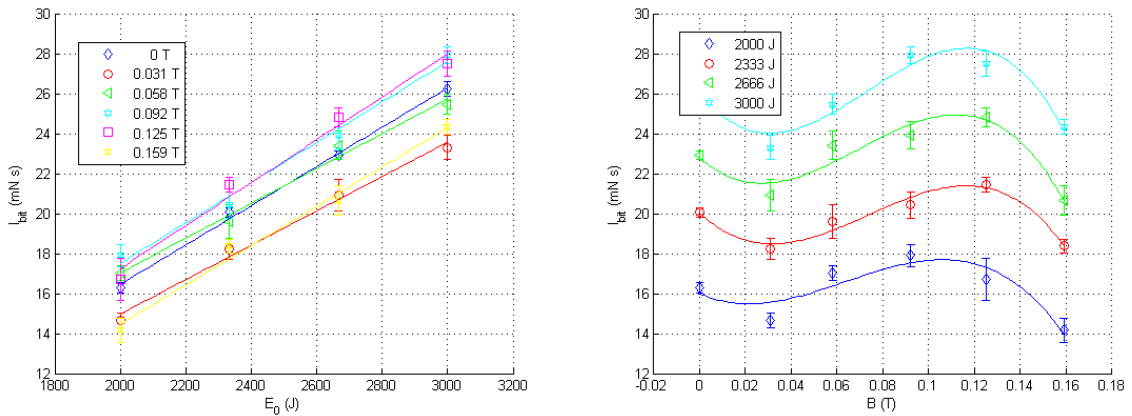
(a) I_{bit} versus initial energy E_0 for each applied B field value. (b) I_{bit} versus applied B field for each initial energy E_0 value.

Figure 13. I_{bit} **trends versus operation parameters.**

evidence of direct summability of the thrust and magnetic coupling phenomena. First it has to be noted that the characteristic times of these events are of different orders of magnitude: the coil operates for almost 0.2 s, while the thruster shot is 0.002 s long. Moreover B field lines distribution should be affected by the presence of a high permeability medium as plasma: the coupling process during thruster firing may be different from that observed during tares measurement. The initial displacement caused by the magnet coil operated alone has the same direction and sense of that produced by thrust: this suggests that the impulse measurements so far discussed are possibly over-estimates. Tares have been calculated measuring the oscillations produced by the magnet without any thruster activity. These values have then been utilized to produce a thrust stand calibration through which all the experimental data have to be re-estimated; the following Fig. 13 (a) and 13 (b) show the impulse bit trends after this calibration. Impulse bit is still linear with E_0 and the current parameter; otherwise Fig. 13 (b), if compared to the corresponding non calibrated thrust stand figure (Fig. 9 (b)), shows a rotation of the impulse bit curves towards lower impulse values; this result becomes straightforward once considered that the larger the magnetic field, the stronger is the coupling between the thrust stand/thruster complex and the vacuum facility's ferromagnetic components, and so the greater is the tare that affects collected data. This is emphasized also by the following Fig. 14 (a): here is depicted the trend of the ratio between calibrated thrust stand impulse bit measurements and the corresponding non calibrated thrust stand impulse bit measurements. For high magnetic field operations it reaches a value well below the unity, down to about 0.75. It is then obvious that also $I_{bit}/(I_{bit})_{B=0}$ and $(I_{bit})_{Reg}/(I_{bit})_{Maecker}$ ratios assume values below
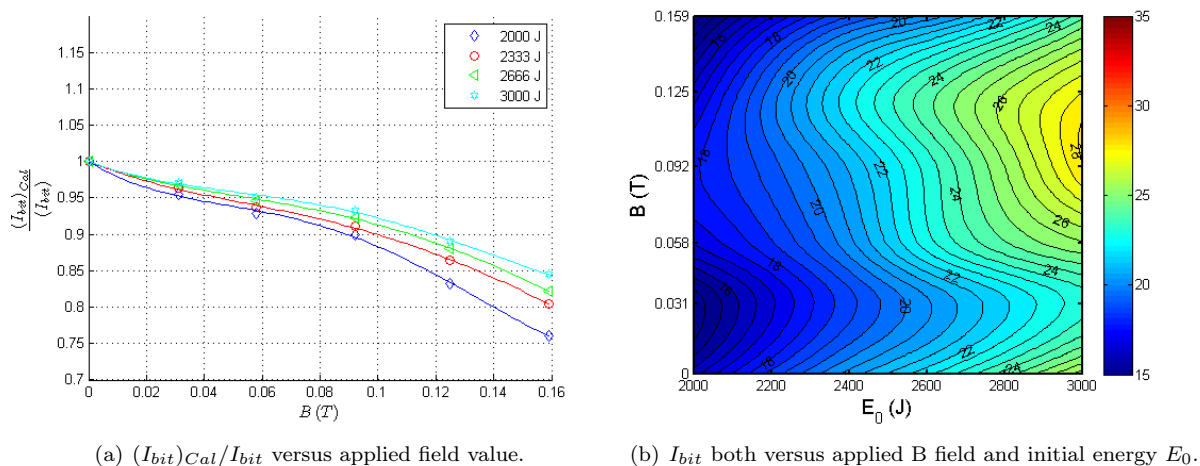

(a) $(I_{bit})_{Cal}/I_{bit}$ versus applied field value.

(b) I_{bit} both versus applied B field and initial energy E_0.

Figure 14.

the unity when high magnetic field values are applied, as in Fig. 15 (a) and Fig. 15 (b). Figures 12 and

(a) $I_{bit}/(I_{bit})_{B=0}$ versus applied field value.

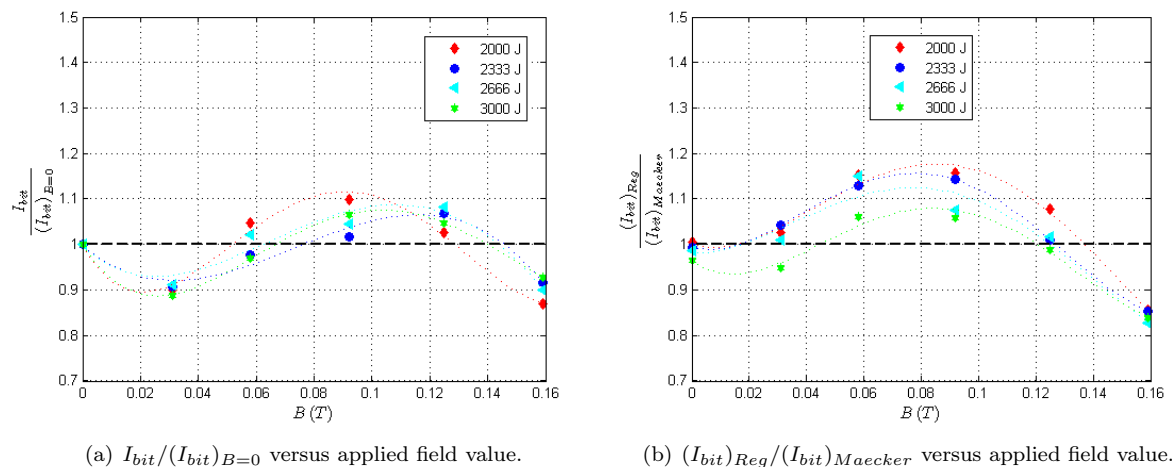(b) $(I_{bit})_{Reg}/(I_{bit})_{Maecker}$ versus applied field value.

Figure 15.

10 presenting $I_{bit}/(I_{bit})_{Maecker}$ and, especially, $I_{bit}/(I_{bit})_{B=0}$ ratios versus the applied field value suggest that the Thrust Stand measurements take into account the applied field effects even without calibration:

if the impulse increments were solely due to magnetic coupling between TS and lab facility, then those ratios should have a linear trend, as that of the coupling itself.

IV. Target

Due to the heavy discrepancy between the two data series, it appears necessary to compare these results with those obtained by means of a different technique, not biased by the magnetic field. The chosen technique is that of a target working as a ballistic pendulum. To achieve a reasonable compromise between the theoretical and the actual device, the target has been designed similar to the thrust stand: it is a double parallel linkage as well, with its motion damped by bars dipped in mercury pots; it has a circular plate mounted on the side exposed to the thruster, big enough to allow the hypothesis that the whole plasma flow collides against it (Fig. 16). The main difference is the material: the target is entirely made of PVC with nylon bolts, in order to have no electromagnetic interaction with the discharge. There are also some minor differences, though, like the oscillation frequency, which is lower, and the suspension bars, which are vertical but guarantee the one-direction motion because of a three-bolt connection to the base plate. This device has the dynamic behavior of the TS, so the same thrust measuring techniques

Figure 16. The Target's Plate after several Mira C firings: radial shading is due to plasma impact burns. The electromagnet can be seen on the right side.

may be applied. However, without a strict evaluation of the energy transferred to the target by the colliding particles, it is not possible to create a unique model of the phenomenon, in order to have a direct absolute thrust measurement. Then the target method requires a taring process, which can be performed applying known impulse values. In order to achieve this tare the TS data have been used: the self-field series for four E_0 values are, in fact, definitely reliable. Therefore a tare coefficient has been sought for: it should be the result of a correspondence between thrust values obtained through
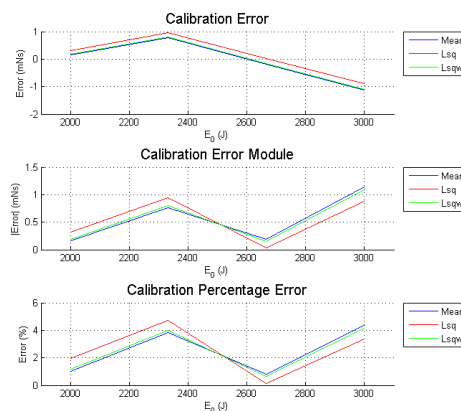

Figure 17. Target calibration error.

the TS technique without the applied field and the values obtained applying the same technique (i.e. exponential regression) to the Target motion curve. It would be desirable for this coefficient to be unique and not dependant on thruster energy: admitting that different energy levels modify the phenomenon and denying the modification for applied-field operation would be a poor assumption; actually it would invalidate the whole Target technique.

Three different coefficient calculation procedures have been carried out: the first one consists in calculating the ratios of impulse values obtained by the two devices for each energy, deriving the coefficient as a raw mean of such ratios; the second method evaluates the coefficient by a least square fitting of the impulse ratios; the third procedure uses a weighted least square technique, which allows to minimize the percent quadratic error, instead of the simple quadratic error. The results given by these different techniques are very close, but those obtained through the last one have been chosen, because it leads to the least value of the percent error on the tare. The green curve Lsqw in Fig. 17 is the one representing the Weighted Least Square results.

V.   Different techniques comparison

Impulse bit values obtained through the target technique are reported in Fig. 18, together with calibrated TS data, as percent deviation from the corresponding results given by the un-calibrated TS. The target results present a deviation always within $\pm$ 10%, with a minimum for the 2333 J energy (within
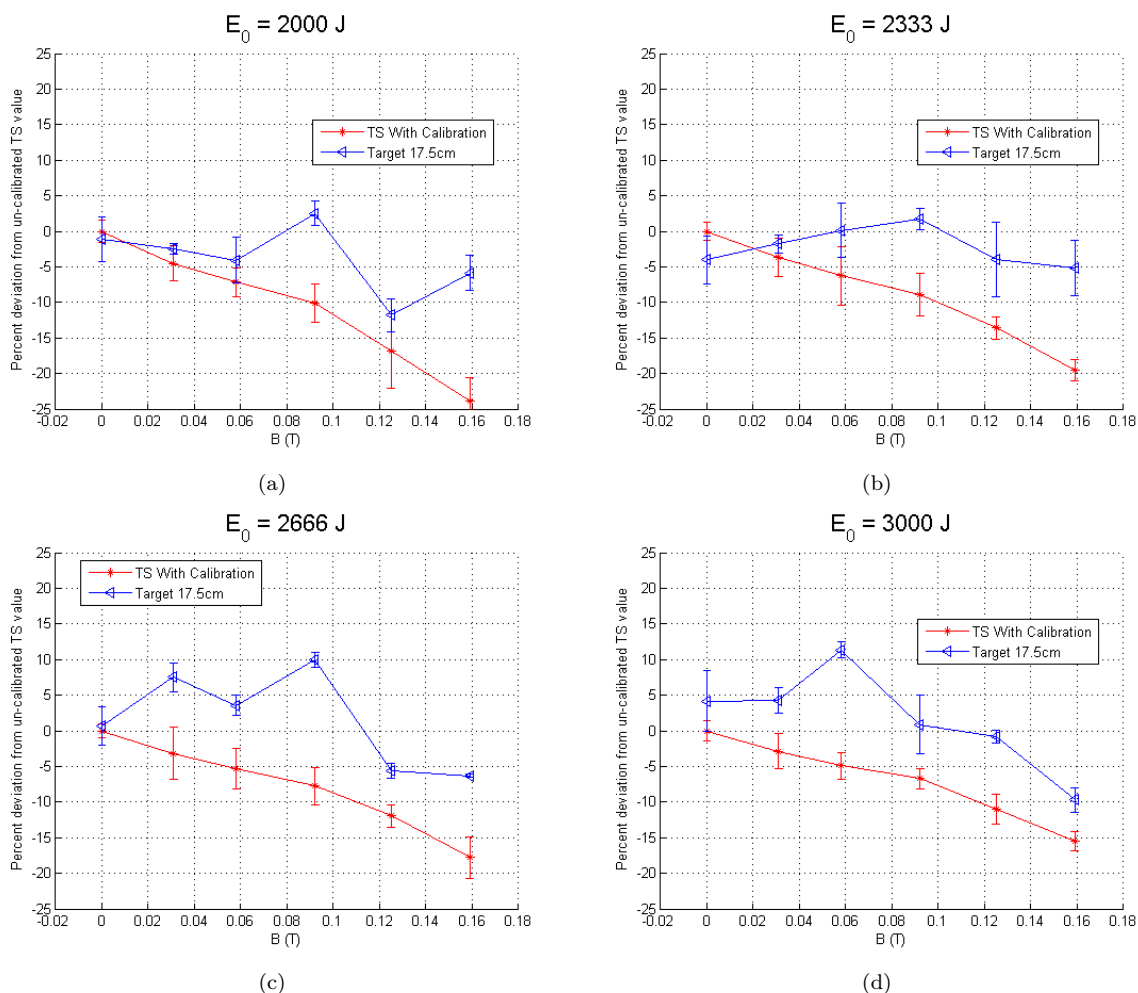

Figure 18. Percent deviation from un-calibrated TS results.

$\pm$ 5%). Moreover the deviation appears not to have a global trend: it floats around zero and shows a definitely decreasing trend only for high applied field values. Conversely, calibrated TS deviation presents only negative values growing in module for increasing magnetic field intensity, since it is obtained by subtracting greater tare values from the reference TS impulse measurements. The accordance between the target and un-calibrated TS techniques supports the idea that the calibration approach leads to underestimates.

A confirmation of the compatibility between target and un-calibrated TS data for low energy values, 2000 J and 2333 J, comes from plotting the impulse values obtained with each taring technique versus the applied field, Fig. 19. It can be noted that the data collected with the Target technique:
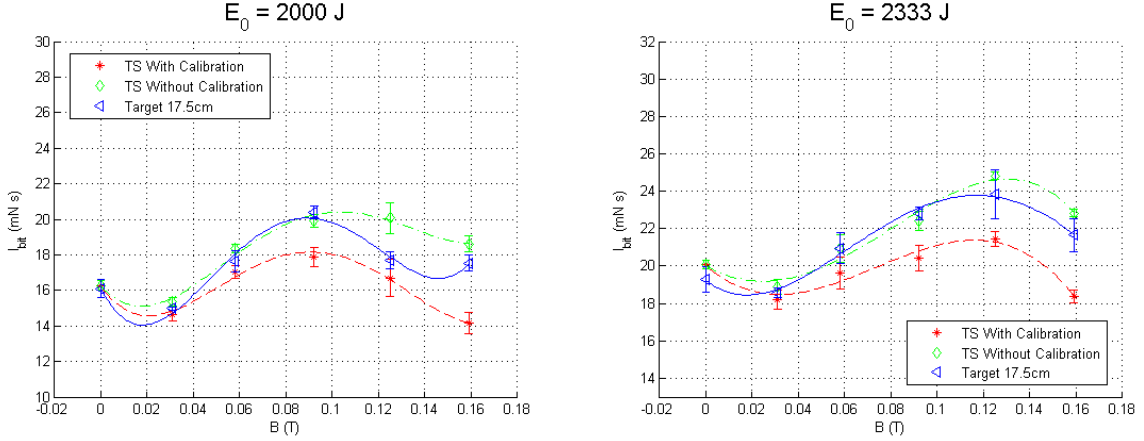

Figure 19. I_{bit} **vs** B **trend for different** E_0 **values. Each figure presents the results obtained through TS (calibrated and non-calibrated) and Target techniques.**

- for lower applied magnetic field show impulse values close to those obtained with the TS without calibration; this indicates that TS calibration leads to an underestimate of the impulse;

- for higher applied magnetic field values show impulse values that are intermediate between those given by uncalibrated and calibrated TS.

Based on these data, it can be supposed that for higher values of the applied field the magnetic coupling effect (between the magnet and the facility), even though appreciable, is however less dramatic than the one suggested by the Thrust Stand calibration technique.

VI.   Concluding Remarks

- High power quasi-steady MPD thruster has been tested both in self-field and applied-field mode.

- Discharge stabilization and discharge duration reduction have been verified as effects of the axial magnetic field application.

- Thrust stand technique for impulse measurement has been analyzed and the Regression method with filtering identified as effective and reliable. Impulse bit results obtained with this technique have been presented.

- Maximum thrust performance enhancement has been found for the applied field value 0.125 T.

- A magnetic coupling effect between the coil and laboratory facility has been verified; subsequent TS calibration has been carried out and new impulse bit measurement results have been obtained.

- In order to override the discrepancy between the two results caused by the magnetic coupling, the indirect target based impulse measurement technique has been adopted. Its results have proven closer to the un-calibrated TS measurements: for lower applied field values the target data series fits the un-calibrated TS one, while for higher applied field intensity target based impulse values are lower, indicating a relevant magnetic coupling effect on un-calibrated TS results.

References

[1]Robert G. Jahn, *Physics of Electric Propulsion*. McGraw-Hill, 1968.

[2]G. Paccani, R. Ravignani, *Sistema di misura della spinta di propulsori MPD*. XII Congresso Nazionale AIDAA, Como, 20–23 July 1993.

[3]T. W. Haag, *Design of a Thrust Stand for High Power Electric Propulsion Devices*. AIAA/ASME/SAE/ASEE 25th Joint Propulsion Conference, Monterey, Canada, July 10–12, 1989.

[4]T. W. Haag, Thrust stand for pulsed plasma thrusters. *Review of Scientific Instruments*, Volume 68, Number 5, May 1997.

[5]S. Orieux, C. Rossi and D. Estève, *Thrust stand for ground tests of solid propellant microthrusters*, *Review of Scientific Instruments*, Volume 73, Number 7, July 2002.

[6]J.H. Gilland, M.L.R. Walker, E.J. Pencil, *Thrust Stand for Applied Field MPD Thrusters*. 29th International Electric Propulsion Conference, Princeton University, October 31 - November 4, 2005.

[7]Y. Kagaya, H. Tahara, T. Yoshikawa, *Effect of Applied Magnetic Nozzle in a Quasi-Steady MPD Thruster*. 28th International Electric Propulsion Conference, Toulouse, France, IEPC-03-031, March 2003.

[8]M. Coletti, A. Balestra, M. Sensini, G. Paccani, *Solid State MPD Thruster with Applied Magnetic Field*, 30th International Electric Propulsion Conference, September 17-20, 2007 / Firenze, Italy.

[9]F. Guarducci, J. Lehnert, G. Paccani, *Quasi-Steady MPD Thrust Stand Analysis*. XX AIDAA Congress, Milano, Italy, June 29 - July 3, 2009.